Phase definition to assess synchronization quality of nonlinear oscillators

Leandro Freitas[*]
Instituto Federal de Educação, Ciência e Tecnologia de Minas Gerais, Campus Betim R. Itaguaçu 595, 32677-562 Betim, Minas Gerais, Brazil

Leonardo A. B. Torres[†] and Luis A. Aguirre[‡]
Departamento de Engenharia Eletrônica e Programa de Pós-Graduação em Engenharia Elétrica, Universidade Federal de Minas Gerais, Avenida Antônio Carlos 6627, 31270-901 Belo Horizonte, Minas Gerais, Brazil

(Received 27 October 2017; revised manuscript received 16 April 2018; published 7 May 2018)

This paper proposes a phase definition, named the vector field phase, which can be defined for systems with arbitrary finite dimension and is a monotonically increasing function of time. The proposed definition can properly quantify the dynamics in the flow direction, often associated with the null Lyapunov exponent. Numerical examples that use benchmark periodic and chaotic oscillators are discussed to illustrate some of the main features of the definition, which are that (i) phase information can be obtained either from the vector field or from a time series, (ii) it permits not only detection of phase synchronization but also quantification of it, and (iii) it can be used in the phase synchronization of very different oscillators.

DOI: 10.1103/PhysRevE.97.052202

I. INTRODUCTION

Synchronization is a ubiquitous phenomenon which has been addressed with different approaches. A common approach is to reduce complex oscillators, such as living beings, to a phase model [1]. This kind of method was successfully used to describe synchronization phenomena in biology [2], chemical oscillators [3], and many others (e.g., [4]), especially in large populations of oscillators.

Another approach is to describe the synchronization phenomenon between coupled complex oscillators without simplifications or reductions. This seems to be more interesting for describing synchronization of chaotic oscillators [5,6] for which dynamical regimes such as complete, phase, lag, intermittent, and generalized synchronization can also be defined [7].

Although each of these two branches of research received considerable attention, a common challenge remains: to define a proper phase variable that can be applied to a wide class of oscillators and should have some desired characteristics. Most papers seem to focus on two main features that a phaselike variable should exhibit: (i) It is a monotonically increasing function of time [7–18] and (ii) it is related to the zero Lyapunov exponent [8–11,19–23] that is associated with the flow direction (e.g., [7,23,24]). The importance of the latter is strengthened by published studies pointing to the fact that a null Lyapunov exponent becomes negative when two coupled oscillators synchronize phases [19]. A phase variable is expected to exist for a general attractor, due to the zero Lyapunov exponent [25], although it may be impossible to explicitly calculate it [11].

The main aim of this paper is to propose a definition for the phase, named the vector field phase (VFP), which is applicable to a large class of oscillators, of any finite dimension. The main features of the VFP are that it increases monotonically with time and has a clear relationship with the flow direction, which corresponds to the zero Lyapunov exponent. Despite its intuitive definition, a phase variable with such a clear connection with the null exponent is not available in the phase synchronization literature.

In order to illustrate the main characteristics of the VFP, examples of assessing phase synchronization of benchmark oscillators are provided. As discussed, the VFP is helpful in evaluating the quality of the synchronization, which is a feature that is not shared by most available phase definitions.

Still, in the vein of validation and testing, a coupling scheme that directly uses the VFP is conceived. The attained results, strict or nonstrict phase locking, confirm that the VFP has the expected features.

This paper is organized as follows. Section II briefly reviews some existing definitions of phase. The proposed definition of the VFP is presented, assuming that the vector field is known, in Sec. III, and not known, in Sec. IV. Numerical examples are provided and discussed in Sec. V and the main conclusions and suggestions for future work are provided in Sec. VI. All mathematical proofs are provided in the Appendix.

II. BACKGROUND

One common way to describe a phase variable, which has led to the concept of isophases [15], is accomplished by defining a Poincaré section $\Gamma_{\mathcal{P}}$ such that the so-called phase value is constant when $\boldsymbol{x} \in \Gamma_{\mathcal{P}}$ and evolves at a constant rate when $\boldsymbol{x} \notin \Gamma_{\mathcal{P}}$, increasing by 2π at each revolution. It is then

[*]Present address: Programa de Pós-Graduação em Engenharia Elétrica, Universidade Federal de Minas Gerais, Avenida Antônio Carlos 6627, 31270-901 Belo Horizonte, Minas Gerais, Brazil; leandro.freitas@ifmg.edu.br
[†]leotorres@ufmg.br
[‡]aguirre@ufmg.br

written as

$$\varphi_a(t) := 2\pi \frac{t - t_k}{t_{k+1} - t_k} + 2\pi k, \quad t_k \leqslant t < t_{k+1}, \tag{1}$$

where t_k is the time of the kth crossing $\Gamma_{\mathcal{P}}$. According to this definition, the phase is piecewise linear and a monotonically increasing function of time. A fundamental drawback is that the phase dynamical behavior within one revolution in state space is totally disregarded [26] since the dynamics in the flow direction is not seen on the Poincaré section.

Consider a projection plane (x,y) on which there is a well-defined center of rotation. In such cases the phase can be defined as [8,19,26–30]

$$\varphi_b(t) := \text{arctan2}(y,x), \tag{2}$$

where $\varphi_b(t) \in [-\pi;\pi)$. The main drawback of this definition arises when the rotation plane is not readily available or it is very difficult to find a proper rotation center as for the Lorenz, funnel Rössler, cord [31], and Li [32] attractors. Specific transformations can be used to help find a rotation center for some systems as for the Lorenz [8] and funnel Rössler [29] attractors. Unfortunately, a general procedure is not yet available.

A phase variable based on the general idea of curvature was proposed in [9,33]:

$$\varphi_c(t) := \text{arctan2}(\dot{y},\dot{x}). \tag{3}$$

Although this proposition solves the problem of finding a rotation center in some cases, the phase variable defined can be nonmonotonic as the curvature signal changes on the attractor, due to curvature inflections. Another aspect is that φ_c will remain constant if the system evolves on a straight-line trajectory.

Other ways to define phase variables are associated with signal processing techniques like the Hilbert transform [16,26,34,35], spectral analysis, and the wavelet transform [12,35–37]. Such definitions assign phase values (e.g., $\varphi_x,\varphi_y,\varphi_z$) to each temporal time series (e.g., x,y,z) and are applied in phase detection problems. However, it is not clear how to decide which variable to use in defining a phase for the system. In general, a well-behaved variable is chosen (a variable that generally exhibits a sinelike temporal behavior), without a clear justification.

Remark 1. There is a distinction between the phase of a signal (one dimensional) and the phase of a trajectory (for an n-dimensional system). This paper addresses only the latter case.

III. DEFINING PHASE BASED ON THE VECTOR FIELD

Consider an oscillator described as $\dot{\boldsymbol{x}} = \boldsymbol{f}(\boldsymbol{x})$, where $\boldsymbol{x} \in X \subseteq \mathbb{R}^n$ is the state vector, $\boldsymbol{f} : X \mapsto \mathbb{R}^n$ a nonlinear function, and $\boldsymbol{x}_0 := \boldsymbol{x}(0) \in X \setminus \{\boldsymbol{x} \in \mathbb{R}^n : \boldsymbol{f}(\boldsymbol{x}) = \boldsymbol{0}\}$ is an initial state that is not an equilibrium point, such that the solution $\gamma(t;\boldsymbol{x}_0)$ exists and is unique. It is assumed that the trajectories converge to an attractor $\Gamma_0 \subseteq X$ as $t \to \infty$. The following definition is proposed.

Definition 1 (vector field phase). For a trajectory $\gamma(t;\boldsymbol{x}_0)$, a VFP ϕ is given by

$$\phi(t) = \phi_0 + \int_{\gamma(t;\boldsymbol{x}_0)} c(\boldsymbol{x})\boldsymbol{f}^{\top}(\boldsymbol{x})d\boldsymbol{x}, \tag{4}$$

where $\phi_0 \in \mathbb{R}$ is an arbitrary constant and $c(\boldsymbol{x})$ is a positive function $c : X \mapsto \mathbb{R}^{*+}$. ■

A similar phase definition has been suggested by Baptista *et al.* [38], but in a context closely related to that of using the returning time to a Poincaré section (1). The main difference is that the phase defined in [38] considers a subspace, with some coherence properties, that is a specific projection of the state space. In this work $\phi_0 = 0$ is used and $c(\boldsymbol{x})$ is chosen as discussed in Sec. III A. It is worth noticing that Definition 1 is intimately connected to the zero Lyapunov exponent, since its computation is effected in the flow direction.

Proposition 1. A VFP (Definition 1) is a monotonic growing function with respect to time. ■

One of the main assumptions of the well-known phase reduction theory [1] is the linear growth rate of the phase variable, i.e., $\phi(t) = \omega t$, with constant ω, for the unperturbed motion. Under certain conditions, $\phi(t)$ is a VFP, as shown below.

Proposition 2. If $\phi_0 = 0$ and $c(\boldsymbol{x}) := \omega/\|\boldsymbol{f}(\boldsymbol{x})\|^2$, the VFP in Definition 1 is $\phi(t) = \omega t$. ■

Therefore, it seems fair to conjecture that if by using the phase reduction approach one can detect synchronization [39,40], the same phenomenon should be possible using a VFP variable. The main drawback of the VFP is that it is not generally possible to describe it as a function of the states, as $\phi(t) \equiv \phi(\boldsymbol{x}(t))$, for an oscillator.[1] This is an essential distinction from most phase definitions.

A. Periodic oscillators

In order to compute the phase using Definition 1 it is necessary to determine $c(\boldsymbol{x})$ and ϕ_0. One possibility for the periodic case is shown in the following, and the chaotic case will be discussed in Sec. III B.

Definition 2. For a given oscillator with limit cycle Γ_0 with period T, $c(\boldsymbol{x})$ can be chosen as

$$c(\boldsymbol{x}) := \frac{2\pi}{\ell\|\boldsymbol{f}(\boldsymbol{x})\|}, \tag{5}$$

where $\ell = \int_0^T \|\boldsymbol{f}(\boldsymbol{x})\|dt$ is the length of Γ_0. ■

Proposition 3. The phase $\phi(t)$ in Definition 1 with $c(\boldsymbol{x})$ given in (5) increases 2π at each rotation on Γ_0. ■

Using Definition 2 and $\phi_0 := 0$, it is possible to write (4) as $\phi(t) = [2\pi/\ell]\int_0^t \|\boldsymbol{f}(\boldsymbol{x}(\tau))\|d\tau$. It becomes clear that this VFP can be interpreted as the integration of the length along the trajectory, since $\|\boldsymbol{f}(\boldsymbol{x}(\tau))\|$ is the instantaneous velocity of the flow. In addition, $2\pi/\ell$ is a normalization factor such that ϕ increases 2π at every revolution.

[1] If $\phi(t) := \phi(\boldsymbol{x}(t))$, then, by (4), the gradient of the ϕ would be $\nabla\phi \equiv c(\boldsymbol{x})\boldsymbol{f}(\boldsymbol{x})$. In this case $\dot{\boldsymbol{x}} = \boldsymbol{f}(\boldsymbol{x})$ is a gradient system and there will be no closed orbits [41]. Then the systems cannot be an oscillator, because there are no limit cycles or unstable periodic orbits.

It is worth noting that ℓ plays an important role concerning the spatial property of recurrence of the phase. It tells us that, after ℓ length units, the system will recur in the state space.

The length along the trajectory was used by Kralemann *et al.* [24] in a phase definition based on a Poincaré section (1) where, instead of the returning time, the length between crossings is computed. Although the technique is useful, a complete reconstruction of the phase dynamics is not possible since it does not convey information about the fast (intracycle) dynamics [24].

It is worth pointing out that Definition 2 does not assume any rotation center or well-behaved curvature on the attractor, but only its periodicity. Hence, the definition holds for any periodic oscillator, in any dimension.

B. Chaotic oscillators

The proposed VFP (Definition 2) presumes a stable limit cycle with a constant length ℓ. For chaotic systems, this length is not constant, since it depends on the trajectory, and an estimate $\hat{\ell}$ should be used instead.

A complete extension to the chaotic case is currently under investigation. However, to illustrate the application of the VFP to chaotic oscillators, the length per revolution will be estimated using a Poincaré section $\Gamma_{\mathcal{P}}$, where $\hat{\ell}_k$ is computed as the trajectory length from the $(k-1)$th and the kth crossing through $\Gamma_{\mathcal{P}}$. In this way, the proposed VFP can be defined for chaotic oscillators.

Remark 2. In the chaotic case, $\hat{\ell}_k$ is the length between two consecutive crossings through $\Gamma_{\mathcal{P}}$ and not the time between crossings, as in the case of φ_a.

The VFP can be defined for other classes of nonperiodic oscillators such as hyperchaotic (Sec. V A 5), non-phase-coherent, and high-dimensional systems. However, the challenge of estimating ℓ remains.

C. Two illustrative examples

In this section the Poincaré and van der Pol oscillators will be used to illustrate some of the main features of the phase definition. More challenging problems are discussed in Sec. V.

1. Poincaré oscillator

Consider the Poincaré system [42]

$$\begin{aligned} \dot{x} &= -\omega y - \lambda(x^2+y^2-p^2)x, \\ \dot{y} &= \omega x - \lambda(x^2+y^2-p^2)y, \end{aligned} \tag{6}$$

with $(\omega,\lambda,p) = (1,0.5,1)$. For (6) the phaselike variable $\varphi_b = \arctan2(y,x)$ [Eq. (2)] is often used [42], for which

$$\frac{d\varphi_b(\boldsymbol{x})}{d\boldsymbol{x}} = \frac{d[\arctan2(y,x)]}{d\boldsymbol{x}} = \begin{bmatrix} \dfrac{-y}{(x^2+y^2)} \\ \dfrac{x}{(x^2+y^2)} \end{bmatrix}. \tag{7}$$

Now for ϕ with Definition 2 the partial derivatives are

$$\begin{bmatrix} \dfrac{\partial\phi}{\partial x} \\ \dfrac{\partial\phi}{\partial y} \end{bmatrix} = \begin{bmatrix} \dfrac{2\pi[-\omega y - \lambda x(x^2+y^2-p^2)]}{\ell\sqrt{[\omega y + \lambda x(x^2+y^2-p^2)]^2 + [\omega x - \lambda y(x^2+y^2-p^2)]^2}} \\ \dfrac{2\pi[\omega x - \lambda y(x^2+y^2-p^2)]}{\ell\sqrt{[\omega y + \lambda x(x^2+y^2-p^2)]^2 + [\omega x - \lambda y(x^2+y^2-p^2)]^2}} \end{bmatrix}. \tag{8}$$

Clearly, the partial derivatives of φ_b and ϕ are not equal. However, for $\boldsymbol{x} \in \Gamma_0$, $x^2+y^2 = p^2$ and $\ell = 2\pi p$, leading to $\nabla_\phi \equiv \partial\phi/\partial\boldsymbol{x} = \partial\varphi_b/\partial\boldsymbol{x}$. In other words, for $\boldsymbol{x} \in \Gamma_0$, $\varphi_b(\boldsymbol{x})$ coincides with the phase ϕ in Definition 1.

A modified version of the Poincaré oscillator is introduced by taking $\omega = \alpha(1-0.9x)$, where the constant α is chosen to achieve the same period as the original oscillator. Hence, the modified Poincaré evolves on the same limit cycle Γ_0, but with a different time evolution (Fig. 1). The evolution of the state on Γ_0 is well represented by all phaselike variables discussed in Sec. II, except φ_a for the modified system.

In this example most of the phaselike variables agree. The main reason for that is the circular shape of Γ_0, yielding a sinusoidal time evolution with constant curvature and length-angle rate. A different scenario is investigated next.

2. van der Pol oscillator

The van der Pol oscillator [43] can be described as

$$\dot{x} = y, \quad \dot{y} = 2\mu y(1-\beta x^2) - \omega^2 x. \tag{9}$$

With $(\mu,\beta,\omega) = (4,1,1)$ the system behaves as an integrate-and-fire oscillator, with acceleration and deceleration regions on the attractor. The time evolution of the phaselike variables are shown in Fig. 2(b), in which the integrate-and-fire regions are clear in all variables except $\varphi_a(t)$ (Poincaré section).

Unlike the previous example, the time evolutions of the phaselike variables (Fig. 2) have different shapes. As expected, $\varphi_a(t)$ disregards the dynamical behavior between crossings of the Poincaré section. The variable $\varphi_c(t)$ is a nonmonotonic function of time, due to the inflections on the curvature of the attractor. On the other hand, $\varphi_b(t)$ and $\phi(t)$ show similar behavior.

The modified oscillator is $\dot{\boldsymbol{x}} = \alpha\boldsymbol{f}(\boldsymbol{x})/\|\boldsymbol{f}(\boldsymbol{x})\|$, where $\boldsymbol{f}(\boldsymbol{x})$ is the vector field in (9) and α is chosen such that both oscillators have the same period. For the modified oscillator, two initial conditions on the limit cycle, $(\boldsymbol{x}_1(0),\boldsymbol{x}_2(0)) \in \Gamma_0$ and $\|\boldsymbol{x}_1(0) - \boldsymbol{x}_2(0)\| < \epsilon$ with $\epsilon \gtrsim 0$, will maintain the initial distance from each other over time, hence $\|\boldsymbol{x}_1(t) - \boldsymbol{x}_2(t)\| = \text{const}\ \forall t$ (see Fig. 2).

In Fig. 2(d) a clear distinction is observed between the VFP and the other phaselike variables: When the evolution

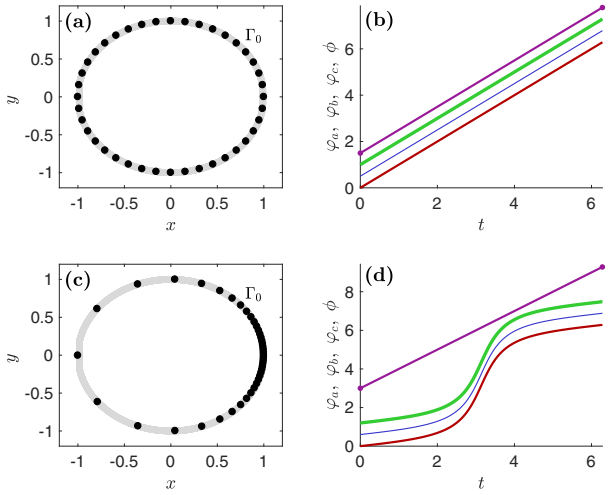

FIG. 1. (a) and (b) Original and (c) and (d) modified Poincaré oscillators: (a) and (c) state space showing evolution on Γ_0 (gray line) and equally time-spaced dots and (b) and (d) phaselike variables vertically displaced for the sake of clarity. Shown, from top to bottom, are φ_a (Poincaré section), φ_b (angle), φ_c (curvature), and ϕ (VFP). The parameters are $(\lambda, p) = (0.5, 1)$, with $\omega = 1$ for the original system, and $\omega = \alpha(1 - 0.9x)$, with $\alpha = 22.646$ for the modified one.

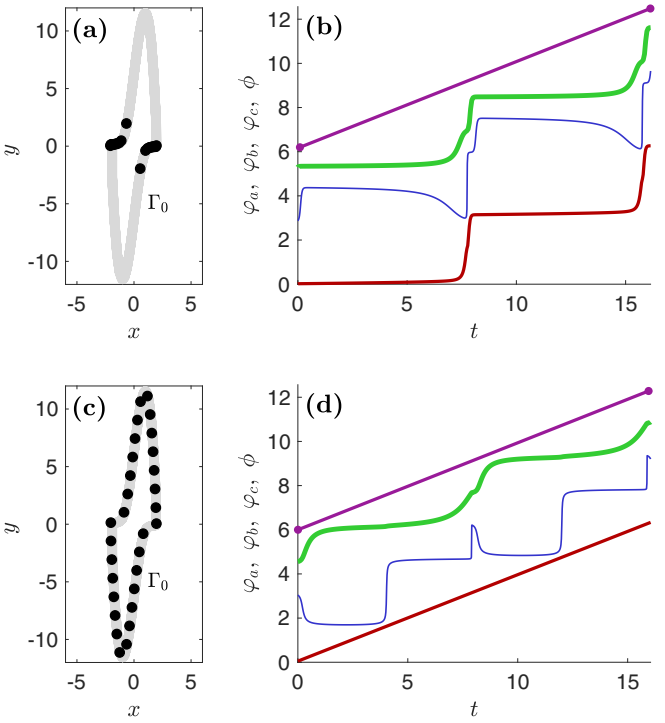

FIG. 2. (a) and (b) Original and (c) and (d) modified van der Pol oscillators with $(\mu, \beta, \omega) = (4, 1, 1)$ and $\alpha = 3.033$: (a) and (c) state space showing evolution on Γ_0 (gray line) and equally time-spaced dots and (b) and (d) phaselike variables vertically displaced for the sake of clarity. Shown, from top to bottom, are φ_a (Poincaré section), φ_b (angle), φ_c (curvature), and ϕ (VFP).

happens at roughly constant speed, the temporal behavior of ϕ is a straight line, showing that in the flow direction, corresponding to the zero Lyapunov exponent, the system evolves at a constant rate. In such a direction there is no local contraction or expansion of a set of initial conditions arbitrarily close to the trajectory.

In Fig. 2(d) φ_b shows some oscillations that are a consequence of the trajectory not being a circle, although the phase should be a straight line. The correct behavior of φ_b in the previous example was due to the perfectly circular trajectory.

Hence the VFP has a consistent interpretation which is based on the dynamics. Some insights concerning phase sync of coupled oscillators can be obtained from the VFP, as shown next.

D. Coupling by phase

Phase synchronization is more efficiently achieved when the coupling signal influences directly the phase dynamics (frequency) [44] as it can be verified in the well-known phase-locked loop [45] or in some applications in complex networks [46,47]. In this section we use this principle to provide further evidence of the suitability of the VFP as a phase measure. To see this, consider an oscillator described as

$$\dot{\boldsymbol{x}} = \boldsymbol{f}(\boldsymbol{x}) + \boldsymbol{g}(\boldsymbol{x})p(\boldsymbol{x},t), \tag{10}$$

where $\boldsymbol{f}, \boldsymbol{g} : \mathbb{R}^n \mapsto \mathbb{R}^n$ are vector functions and $p : \mathbb{R}^n \times \mathbb{R} \mapsto \mathbb{R}$ is an external signal that drives the system to phase synchronization with another oscillator. From the previous discussion, if $\boldsymbol{g}(\boldsymbol{x})$ and $\boldsymbol{f}(\boldsymbol{x})$ are collinear for all $\boldsymbol{x} \in X$, $p(\boldsymbol{x},t)$ will be most effective in changing the phase dynamics. On the contrary, if $\boldsymbol{g}(\boldsymbol{x}) \perp \boldsymbol{f}(\boldsymbol{x})$, phase synchronization can be very difficult or even impossible.

The collinearity between the vector functions can be trivially achieved by choosing $\boldsymbol{g}(\boldsymbol{x}) \equiv \boldsymbol{f}(\boldsymbol{x})$. In this way, aside from the direct influence on the (VFP) phase dynamics, furthermore, the signal $p(\boldsymbol{x},t)$ will drive the rhythm of the oscillator, i.e., it will make a reparametrization of time (see [48], Sec. 1.4). For instance, a constant value $p(\boldsymbol{x},t) \equiv p_0$ will change the period of an oscillation from T to $(1 + p_0)T$, directly.

Unlike other phase definitions, the VFP provides insight into how to effectively actuate the system, at each point in state space in order to directly influence the oscillator period. This is further investigated next.

1. A VFP-based coupling scheme

Consider two coupled periodic oscillators, each one described as in (10), with $\boldsymbol{g}_i(\boldsymbol{x}_i) \equiv \boldsymbol{f}_i(\boldsymbol{x}_i)$ and $p(\boldsymbol{x}_i,t)$ a drive signal proportional to the phase error in order to attain phase synchronization. With the VFP variables ϕ_1 and ϕ_2 as described in Definitions 1 and 2, and taking the phase difference $\psi := \phi_1 - \phi_2$, it is possible to write the equations of the coupled oscillators as

$$\begin{aligned}
\dot{\boldsymbol{x}}_1 &= \boldsymbol{f}_1(\boldsymbol{x}_1) - \beta\varepsilon \boldsymbol{f}_1(\boldsymbol{x}_1)\psi, \\
\dot{\boldsymbol{x}}_2 &= \boldsymbol{f}_2(\boldsymbol{x}_2) + \varepsilon \boldsymbol{f}_2(\boldsymbol{x}_2)\psi, \\
\dot{\psi} &= \frac{2\pi}{\ell_1}\|\boldsymbol{f}_1(\boldsymbol{x}_1) - \beta\varepsilon \boldsymbol{f}_1(\boldsymbol{x}_1)\psi\| \\
&\quad - \frac{2\pi}{\ell_2}\|\boldsymbol{f}_2(\boldsymbol{x}_2) + \varepsilon \boldsymbol{f}_2(\boldsymbol{x}_2)\psi\|,
\end{aligned} \tag{11}$$

with $\boldsymbol{x}_i \in \mathbb{R}^{n_i}$ and $\boldsymbol{f}_i : \mathbb{R}^{n_i} \mapsto \mathbb{R}^{n_i}$ $i \in \{1,2\}$. In the case of bidirectional coupling $\beta = 1$; otherwise $\beta = 0$. Let $\boldsymbol{x} := [\boldsymbol{x}_1^\top, \boldsymbol{x}_2^\top, \psi]^\top$ be the state vector of the overall system. The following assumptions are made.

Assumption 1. Each uncoupled oscillator settles to a minimal compact ω-limit set Γ_i (attractor).

Assumption 2. The initial states $x_{0,i} := x_i(0)$ are on the corresponding attractor, $x_{0,i} \in \Gamma_i$.

Assumption 3. The initial phase difference $\psi_0 := \psi(0) = \phi_1(0) - \phi_2(0) \in (-1/\varepsilon, 1/\varepsilon)$.

Since the attractor is a bounded set, the condition

$$v_{i,\min} < \|\boldsymbol{f}_i(\boldsymbol{x}_i)\| < v_{i,\max} \tag{12}$$

will hold for all $\boldsymbol{x}_i \in \Gamma_i \; \forall i \in \{1,2\}$.

The proposed framework (11) can be used to analyze strict and nonstrict phase-locking conditions (see [49], p. 8), respectively given by

$$\lim_{t\to\infty} \psi(t) = \psi_{\text{dev}}, \tag{13}$$

$$\psi_{\min} \leqslant \psi(t) \leqslant \psi_{\max} \; \forall t > t_0, \tag{14}$$

where t_0, ψ_{dev}, $\psi_{\min}$, and $\psi_{\max}$ are constant values. Following Vorotnikov [50] and Miroshnik [51], the partial stability analysis is done with respect to the state $\psi(t)$, and not to the whole state space, and is therefore called ψ stability [50].

It will be convenient to define partial stability using concepts of attracting sets (submanifolds), which allows the use of geometric control techniques to derive sufficient conditions to ensure local ψ stability [51].

Definition 3. For the system (11) if for all $\boldsymbol{x}_0 \in \mathcal{Z}$ and $t \geqslant t_0$, $\boldsymbol{x}(t;\boldsymbol{x}_0) \in \mathcal{Z}$, $\mathcal{Z}$ is said to be positively invariant. ■

We are particularly interested in invariant sets where ψ remains bounded, nonstrict phase locking (14), or where it converges asymptotically to a constant value, strict phase locking (13). It is interesting to analyze the motion in the neighborhood of $\mathcal{Z}$ which is an open set $\mathcal{E}(\mathcal{Z})$ such that $\mathcal{E}(\mathcal{Z}) \supset \mathcal{Z}$. We introduce the distance from an arbitrary point $\boldsymbol{x} \in \mathcal{E}(\mathcal{Z})$ to $\mathcal{Z}$ as

$$\text{dist}(\boldsymbol{x}, \mathcal{Z}) = \inf_{\boldsymbol{x}^* \in \mathcal{Z}} \|\boldsymbol{x} - \boldsymbol{x}^*\|. \tag{15}$$

Definition 4 (from [51]). The set $\mathcal{Z}$ is called an attracting submanifold of the system (11) when it is invariant and uniformly attractive, i.e., there exists a neighborhood $\mathcal{E}(\mathcal{Z})$ such that for all $\boldsymbol{x}_0 \in \mathcal{E}(\mathcal{Z})$,

$$\lim_{t\to\infty} \text{dist}(\boldsymbol{x}(t;\boldsymbol{x}_0), \mathcal{Z}) = 0, \tag{16}$$

uniformly in $\mathcal{E}(\mathcal{Z})$. ■

These concepts can be used to analyze the boundedness of $\psi(t)$. The following section shows sufficient conditions to achieve strict and nonstrict phase locking.

Remark 3. The coupled system (11) can be rewritten as

$$\begin{aligned} \dot{\phi}_1 &= v_1(t)|1 - \beta\varepsilon\psi|, \\ \dot{\phi}_2 &= v_2(t)|1 + \varepsilon\psi|, \\ \dot{\psi} &= \phi_1 - \phi_2, \end{aligned} \tag{17}$$

where $v_i(t) = (2\pi/\ell_i)\|\boldsymbol{f}_i[\boldsymbol{x}_i(t)]\| \geqslant 0$, for $i \in \{1,2\}$, are bounded (12) exogenous signals. For $|\psi| < 1/\varepsilon$ it is possible to write $\dot{\psi} = [v_1(t) - v_2(t)] - \varepsilon[\beta v_1(t) - v_2(t)]\psi$, resembling the well-known phase reduction [1] analysis. ■

2. *Sufficient conditions for phase locking*

For two coupled oscillators described by (11) the following theorem holds.

Theorem 1. For two bidirectionally ($\beta = 1$) coupled oscillators (11) with a constant coupling strength $\varepsilon := \varepsilon_0$ and considering Assumptions 1–3, the nonstrict phase-locking condition (14) is ensured with

$$\psi_{\min} = \frac{1}{\varepsilon_0}\left(\frac{\ell_2 v_{1,\min} - \ell_1 v_{2,\max}}{\ell_2 v_{1,\min} + \ell_1 v_{2,\max}}\right), \tag{18}$$

$$\psi_{\max} = \frac{1}{\varepsilon_0}\left(\frac{\ell_2 v_{1,\max} - \ell_1 v_{2,\min}}{\ell_2 v_{1,\max} + \ell_1 v_{2,\min}}\right) \tag{19}$$

for some finite positive t_0. ■

In the special case where the norm of the vector field is constant for both oscillators, i.e., $\|\boldsymbol{f}_i(\boldsymbol{x}_i)\| = v_i \; \forall \boldsymbol{x}_i \in \Gamma_i$ for $i \in \{1,2\}$, the strict phase-locking condition (13) is ensured with

$$\psi_{\text{dev}} = \frac{1}{\varepsilon_0}\left(\frac{\ell_2 v_1 - \ell_1 v_2}{\ell_2 v_1 + \ell_1 v_2}\right). \tag{20}$$

Similar results for the unidirectionally coupled oscillators ($\beta = 0$) can be derived, with the benefit of some relaxation of the Assumption 3 (initial phase difference), which can be replaced by the following.

Assumption 4. If $\beta = 0$, the initial phase difference $\psi_0 := \psi(0) = \phi_1(0) - \phi_2(0) \in (-1/\varepsilon, \infty)$.

Results for the nonstrict and strict phase-locking conditions are, respectively, presented next.

Theorem 2. For two unidirectionally ($\beta = 0$) coupled oscillators (11) with a constant coupling strength $\varepsilon := \varepsilon_0$ and considering Assumptions 1, 2, and 4, the nonstrict phase-locking condition (14) is ensured with

$$\psi_{\min} = \frac{1}{\varepsilon_0}\left(\frac{\ell_2 v_{1,\min}}{\ell_1 v_{2,\max}} - 1\right), \tag{21}$$

$$\psi_{\max} = \frac{1}{\varepsilon_0}\left(\frac{\ell_2 v_{1,\max}}{\ell_1 v_{2,\min}} - 1\right) \tag{22}$$

for some finite positive t_0. ■

In the special case where $\|\boldsymbol{f}_i(\boldsymbol{x}_i)\| = v_i \; \forall \boldsymbol{x}_i \in \Gamma_i$ for $i \in \{1,2\}$, the strict phase-locking condition (13) is ensured with

$$\psi_{\text{dev}} = \frac{1}{\varepsilon_0}\left(\frac{\ell_2 v_1}{\ell_1 v_2} - 1\right). \tag{23}$$

Some applications of these results are presented in Sec. V.

IV. DEFINING PHASE BASED ON OBSERVABLES

The present section shows how to estimate the VFP without knowledge of the vector field. Without loss of generality, and with an eye on applications, it is assumed that the data are regularly sampled at instants t_k, $k = 0,1,\ldots$.

Consider an observable $s_k = h[\boldsymbol{x}(t_k)] \in \mathbb{R}$ from a nonlinear oscillator where $h : \mathbb{R}^n \mapsto \mathbb{R}$ is a measuring function that acts on the original state space. From the sequence $\{s_k\}$ it is possible to reconstruct an embedding space using, say,

delay coordinates $\boldsymbol{x}_k \equiv [s_k, s_{k-\tau}, \ldots, s_{k-\tau(d-1)}]^\top$, where τ is the delay time and d is the embedding dimension. Takens' theorem [52] ensures that if d is sufficiently large, the attractors in the reconstructed and original spaces are diffeomorphic. Hence, given $\boldsymbol{x}_k$, the reconstructed vector field can be locally estimated as

$$\hat{\boldsymbol{f}}(\boldsymbol{x}_k) = \frac{\boldsymbol{x}_k - \boldsymbol{x}_{k-1}}{t_k - t_{k-1}}. \tag{24}$$

Recalling that the VFP can be interpreted as the length along the flow, its estimate becomes

$$\hat{\phi}_k = \phi_0 + \frac{2\pi}{\ell} \sum_{i=1}^{k} \|\boldsymbol{x}_i - \boldsymbol{x}_{i-1}\|. \tag{25}$$

The cost of computing (25) is similar to the explicit phase definitions presented so far. In Sec. V some numerical results on assessing phase synchronization with (25) are presented.

Coupling without the vector field

The coupling scheme presented in Sec. III D can be applied without the full knowledge of the vector field. Consider the two nonlinear oscillators

$$\begin{aligned} \dot{\boldsymbol{x}}_1 &= \boldsymbol{f}_1(\boldsymbol{x}_1) - \beta\varepsilon \boldsymbol{p}_1(t), \\ \dot{\boldsymbol{x}}_2 &= \boldsymbol{f}_2(\boldsymbol{x}_2) + \varepsilon \boldsymbol{p}_2(t), \end{aligned} \tag{26}$$

where the aim is the design of the vector functions $\boldsymbol{p}_1$ and $\boldsymbol{p}_2$ in order to phase synchronize both systems. It is considered that the vector fields $\boldsymbol{f}_1(\boldsymbol{x}_1)$ and $\boldsymbol{f}_2(\boldsymbol{x}_2)$ are unknown, but the state variables are available. To address more practical cases, we consider $\boldsymbol{p}_1(t)$ and $\boldsymbol{p}_2(t)$ as piecewise constant vector functions whose values can change only at the sampling instants t_k.

Following the procedure adopted in Sec. III D and considering the phase estimate (25), it is possible to implement the coupling scheme with

$$\begin{aligned} \psi_k &= \psi_{k-1} + \left[\frac{2\pi}{\ell_1}\|\hat{\boldsymbol{f}}_1(\boldsymbol{x}_{1k})\| - \frac{2\pi}{\ell_2}\|\hat{\boldsymbol{f}}_2(\boldsymbol{x}_{2k})\|\right]\Delta t_k, \\ \boldsymbol{p}_{1k} &= \hat{\boldsymbol{f}}_1(\boldsymbol{x}_{1k})\psi_k, \quad \boldsymbol{p}_1(t) = \boldsymbol{p}_{1k}, \ t \in [t_k, t_{k+1}), \\ \boldsymbol{p}_{2k} &= \hat{\boldsymbol{f}}_2(\boldsymbol{x}_{2k})\psi_k, \quad \boldsymbol{p}_2(t) = \boldsymbol{p}_{2k}, \ t \in [t_k, t_{k+1}), \end{aligned} \tag{27}$$

where $\Delta t_k = t_k - t_{k-1}$ is the sampling time and $\hat{\boldsymbol{f}}_i(\boldsymbol{x}_{ik})$ are estimated by (24) based on the state vector of the ith oscillator. In comparison with (11), notice that each term inside the norms in (27) does not include the external signals $\boldsymbol{p}_1$ and $\boldsymbol{p}_2$. The reason is that, because the estimate (24) is based on the states, the external influences are already considered, e.g., $\hat{\boldsymbol{f}}_i(\boldsymbol{x}_{ik}) \approx \boldsymbol{f}_i(\boldsymbol{x}_i(t_k)) + \boldsymbol{p}_i(t_k)$.

V. NUMERICAL RESULTS

In this section the VFP is used to assess phase synchronization. It is shown that the VFP can provide additional information beyond detecting phase synchronization even if the vector field is not known.

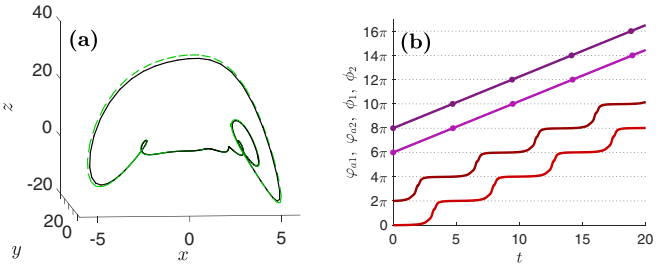

FIG. 3. Results for the cord oscillators (28): (a) steady-state evolution of uncoupled ($\varepsilon = 0$) oscillators 1 (solid black line) and 2 (dashed green line) and (b) phase variables, from top to bottom, φ_{a1}, φ_{a2}, ϕ_1, and ϕ_2.

A. Assessing phase synchronization

Consider two coupled nonidentical cord systems [31]

$$\begin{aligned} \dot{x}_{1,2} &= -y_{1,2} - z_{1,2} - a x_{1,2} + aF + \varepsilon(x_{2,1} - x_{1,2}), \\ \dot{y}_{1,2} &= x_{1,2} y_{1,2} - b_{1,2} x_{1,2} z_{1,2} - y_{1,2} + G, \\ \dot{z}_{1,2} &= b_{1,2} x_{1,2} y_{1,2} + x_{1,2} z_{1,2} - z_{1,2}, \end{aligned} \tag{28}$$

where the subindices indicate the oscillator; $(a, F, G) = (0.258, 8.0, 1.0)$ are the same for both oscillators and $b_1 \neq b_2$. First, $(b_1, b_2) = (3.85, 3.80)$, for which both systems are in period-1 regimes. The second result corresponds to $(b_1, b_2) = (4.45, 4.25)$. All simulations use the Runge-Kutta fourth-order method with an integration time step of 0.01.

1. Periodic cord oscillator

Figure 3(a) shows the limit cycles for both uncoupled periodic oscillators (28). The attractors do not have a single rotation center, or even a single rotation direction, and present curvature inflections. The rotation on the (y, z) plane changes its direction halfway through the cord. Thus, it is hardly possible to define a monotonic growing phaselike variable by means of curvature or angle measurement (i.e., some transformation would be needed). One can define a phaselike variable φ_a with the Poincaré section $\Gamma_{\mathcal{P}} = \{\boldsymbol{x} \in X | x = 0, \dot{x} > 0\}$, but with no dynamical information about the phase evolution between consecutive crossings of $\Gamma_{\mathcal{P}}$.

By contrast, the VFP can successfully represent the irregular evolution on the limit cycle that resembles a kind of integrate-and-fire oscillator. Figure 3(b) shows that the VFP provides this information, where the almost horizontal part of $\phi(t)$ corresponds to the evolution on the cord (integrating) and the quick increase corresponds to the evolution on the wings (firing). As expected, the phaselike variable φ_a does not convey any detailed information about the oscillations.

When the oscillators are (mutually) coupled, it is possible to identify the nonstrict phase-locking (see [49], p. 8) regime by verifying $|\phi_1(t) - \phi_2(t)| < \text{const}$. Figure 4 shows the phase difference $\Delta\varphi_a$ and $\Delta\phi$ for six values of coupling strength. Note that the amplitude of the fluctuations of $\Delta\phi$, the energy of $\Delta\phi(t)$, decays with increasing ε, which reveals different levels of synchronization. A high variance of the signal indicates that the systems are almost losing the phase-locking regime. On the other hand, small fluctuations of the phase difference

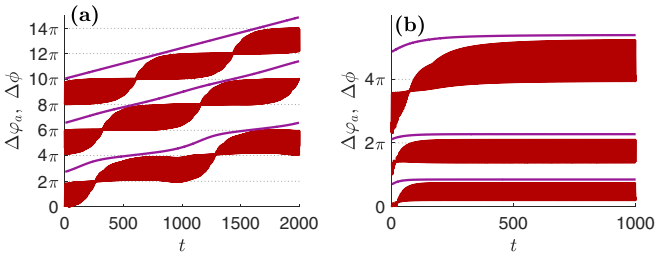

FIG. 4. Results for the cord oscillators (28): time evolution of the phase differences $\Delta\varphi_a$ and $\Delta\phi$ of mutually coupled systems for six values of coupling strengths, from top to bottom, (a) $\varepsilon = 0, 1\times10^{-3}$, and 5×10^{-3} and (b) $\varepsilon = 1\times10^{-2}$, 2×10^{-2}, and 3×10^{-2}. Some transient regime at the beginning ($t < 400$) is shown in (b).

(VFP) indicate a tight sync state. This sort of detail is absent in $\Delta\varphi_a$.

2. Chaotic cord oscillator

As for the periodic case, two coupled chaotic cord oscillators (28), with $(b_1,b_2) = (4.45,4.25)$, can attain the synchronization regime by gradually increasing ε (Fig. 5). The evolution of $\Delta\varphi_a$ is very similar in all synchronized cases [Fig. 6(a)] and it would be difficult to quantify the quality of synchronization in each case. Contrary to this, $\Delta\phi$ reveals differences.

To emphasize this point, the energy of $\Delta\phi(t)$, measured by its variance, is shown in Fig. 6(b) for various values of ε. The phase difference based on the VFP can reveal different levels of synchronization, where a low variance of $\Delta\phi$ indicates high-quality phase synchronization.

To explore this point further, a random noise ($\mu = 0, \sigma = 0.05$) was added to the first state equation of both oscillators. Figure 7 shows that the noise caused more phase slips on those cases where the variance of the VFP was high in the noiseless case [see Fig. 6(b)]. For $\varepsilon = 1\times10^{-3}$, the variance of the VFP was very low and the added noise did not cause any phase slips.

Such details are not conveyed by φ_a in general. One can argue that the average value of $\Delta\varphi_a$ can also convey a measure of the quality of synchronization. That is true when dealing with very similar systems, when the Poincaré sections of both systems are defined in the "same location" in the state space and thus the values of reference of the phase variables are the same and can be compared. In contrast, dealing with very

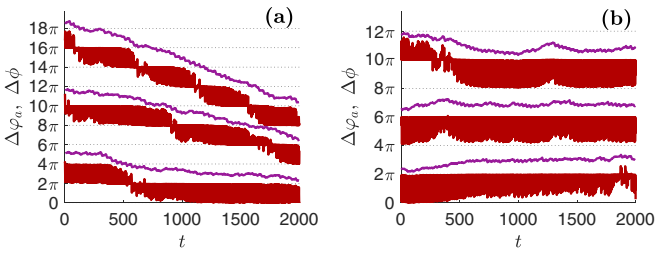

FIG. 5. Results for chaotic cord oscillators (28): time evolution of the phase differences $\Delta\varphi_a$ and $\Delta\phi$ of mutually coupled systems for six values of coupling strengths, from top to bottom, (a) $\varepsilon = 1\times10^{-5}$, 5×10^{-5}, and 1×10^{-4} and (b) $\varepsilon = 5\times10^{-4}$, 7×10^{-4}, and 1×10^{-3}. Some transient regime ($t < 500$) is shown in (b).

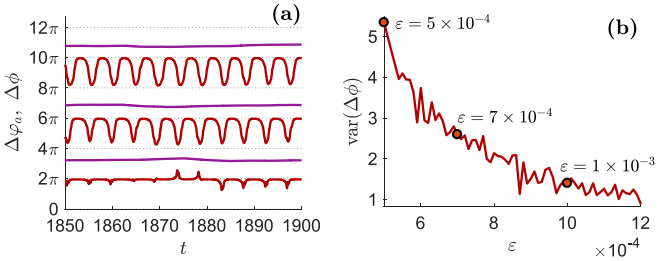

FIG. 6. Results for chaotic cord oscillators in a steady state (28): (a) details of $\Delta\varphi_a$ and $\Delta\phi$ of mutually coupled systems in the phase synchronization regime for three values of coupling strengths, from top to bottom, $\varepsilon = 5\times10^{-4}, 7\times10^{-4}$, and 1×10^{-3} and (b) variance of $\Delta\phi$ according to the coupling strength.

different systems, the value of the phase difference becomes meaningless, susceptible to the arbitrariness of the choice of the Poincaré section, since the phase values of each system are not comparable. This point is discussed next.

3. Coupling very different systems

Many real-world phenomena involving phase synchronization occur between very different systems. The influence of the sun on life cycles on earth, the interaction between foodwebs, and the synchronization between neurons in the brain are some examples.

Here the VFP is used to assess phase synchronization of a cord system [31] mutually coupled with the modified Hodgkin-Huxley model [53]. Both uncoupled oscillators behave chaotically and have different dimensions. The parameters of the cord system (28) are $(a,b,F,G) = (0.258,4.45,8.0,1.0)$. For the modified Hodgkin-Huxley model, the same parameters as in [54] are used, except the values $s_d = 0.25\ \text{mV}^{-1}$, $s_r = 0.25\ \text{mV}^{-1}$, $V_l = -60$ mV, $T = 12\,^{\circ}$C, and $\xi(t) = 0\,\forall t$. The cord system was simulated with a multiplying timescale factor of $\alpha = 0.004$ in order to make the timescales compatible. Simulations use the fourth-order Runge-Kutta model with an integration step of 0.1.

The systems are mutually coupled with the ordinary diffusive (normalized) scheme as

$$\begin{bmatrix} \dot{V} \\ \dot{a}_r \\ \dot{a}_{sd} \\ \dot{a}_{sr} \end{bmatrix} = \boldsymbol{f}_1(V,a_r,a_{sd},a_{sr}) + \varepsilon \begin{bmatrix} 0 \\ 0 \\ (\bar{z} - \bar{a}_{sd})\sigma_{a_{sd}} + \mu_{a_{sd}} \\ 0 \end{bmatrix}, \quad (29)$$

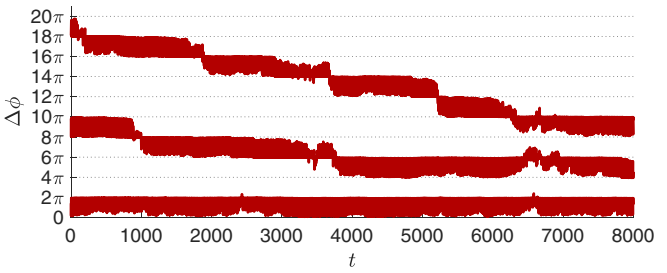

FIG. 7. Phase difference $\Delta\phi$ of mutually coupled chaotic cord oscillators (28) with noise (see the text) for three values of coupling strength, from top to bottom, $\varepsilon = 5\times10^{-4}, 7\times10^{-4}$, and 1×10^{-3}.

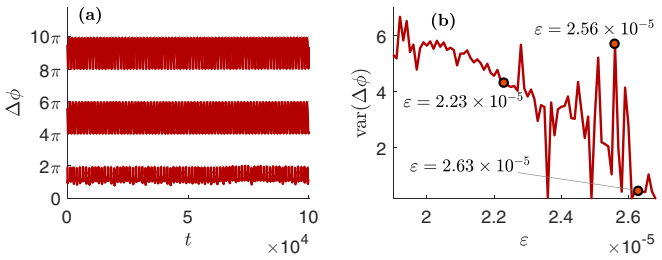

FIG. 8. Results for a chaotic cord oscillator mutually coupled with a chaotic modified Hodgkin-Huxley model (29): (a) time evolution of $\Delta\phi$ for three values of coupling strengths, from top to bottom, $\varepsilon = 2.23 \times 10^{-5}$, 2.56×10^{-5}, and 2.63×10^{-5}, all in the phase synchronization regime, and (b) variance of $\Delta\phi$ according to the coupling strength.

$$\begin{bmatrix} \dot{x} \\ \dot{y} \\ \dot{z} \end{bmatrix} = \boldsymbol{f}_2(x,y,z) + \varepsilon \begin{bmatrix} 0 \\ 0 \\ (\bar{a}_{sd} - \bar{z})\sigma_z + \mu_z \end{bmatrix}, \qquad (30)$$

where $\boldsymbol{f}_1 : \mathbb{R}^4 \mapsto \mathbb{R}^4$ and $\boldsymbol{f}_2 : \mathbb{R}^3 \mapsto \mathbb{R}^3$ are the vector fields of the uncoupled oscillators; the bars on $\bar{a}_{sd}$ and $\bar{z}$ indicate that a normalization (standard score) with respect to the uncoupled system was taken; μ and σ are constants that represents the average and standard deviation of the subscripted variable. These values normalize the magnitudes of the coupled variables.

For the case shown in Fig. 8, the relationship between ε and the variance of the VFP is not as clear as in the previous case (Fig. 6), due to the heterogeneity of the oscillators. Notice how the VFP variance for the second value of ε is greater than for the first one despite the stronger coupling.

However, the same interpretation for what concerns the synchronization quality is possible. When random noise is added to the state equations of $\dot{a}_{sd}$ and $\dot{z}$, the higher the variance of the VFP in the noiseless case, the more phase slips occur (Fig. 9). This shows that the insights provided by the VFP are consistent and can be applied in a wide variety of problems.

4. Assessing phase sync without the vector field

As shown in Sec. IV, the VFP can be defined based on observables. Consider the coupled chaotic cord oscillators

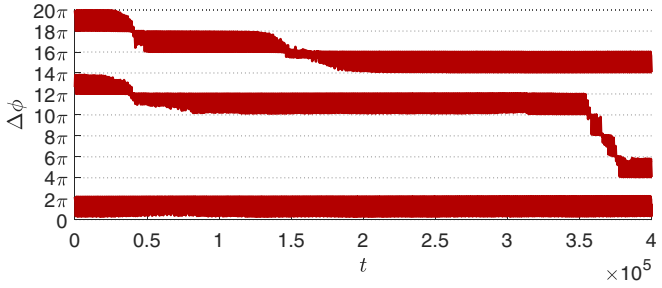

FIG. 9. Phase difference $\Delta\phi$ of the mutually coupled cord and the modified Hodgkin-Huxley oscillators (29), where a random noise of zero mean and 0.05% of the standard deviation of the respective variable was added to the corresponding state equation, for, from top to bottom, $\varepsilon = 2.23 \times 10^{-5}$, 2.56×10^{-5}, and 2.63×10^{-5}.

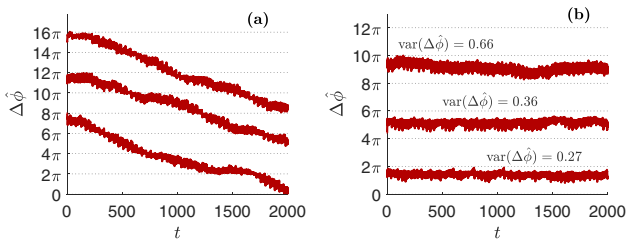

FIG. 10. Results for chaotic cord oscillators without using the system of equations (28): phase difference $\Delta\hat{\phi}$ computed with (25) and delay embedding. The mutually coupled systems are with, from top to bottom, (a) $\varepsilon = 1 \times 10^{-5}$, 5×10^{-5}, and 1×10^{-4} and (b) $\varepsilon = 5 \times 10^{-4}$, 7×10^{-4}, and 1×10^{-3}.

(28), where only the x variable of each system is available. Choosing the embedding parameters as in Ref. [31], with dimension $d = 4$ and delay $\tau = 0.84$, it is possible to define the VFP without the equations.

Figure 10 shows $\Delta\hat{\phi}$ for the same values of ε shown in Fig. 5(b). Comparing both figures, it is possible to note some differences in the microdynamics, perhaps due to the reconstruction via delay embedding. However, the main features concerning phase synchronization phenomena are qualitatively similar, including the previous discussion about the quality of the phase synchronization regime. Note that the higher coupling strength in Fig. 10 corresponds to a lower variance of the VFP.

5. Assessing phase sync on coupled hyperchaotic systems

The same insights presented so far can be obtained by applying the VFP to other classes of nonperiodic systems. Consider two mutually coupled hyperchaotic Rössler oscillators as $\dot{\boldsymbol{x}}_{1,2} = \boldsymbol{f}_{1,2}(\boldsymbol{x}_{1,2}) + \varepsilon(\boldsymbol{x}_{2,1} - \boldsymbol{x}_{1,2})$, where the subindices denote different systems, with

$$\boldsymbol{f}_1 = \begin{bmatrix} -y - z \\ x + 0.25y + w \\ 3 + xz \\ -0.5z + 0.05w \end{bmatrix}, \quad \boldsymbol{f}_2 = \begin{bmatrix} -y - z \\ x + 0.255y + w \\ 3 + xz \\ -0.5z + 0.05w \end{bmatrix}. \qquad (31)$$

When dealing with hyperchaotic systems an important challenge is to estimate ℓ. Here the cross section given by $\mathcal{S} = \{\boldsymbol{x} \in \mathbb{R}^4 | x < -15, y = 0, \dot{y} < 0\}$ is used to compute $\hat{\ell}$ at each revolution. Note that there is no (topological) guarantee that $\mathcal{S}$ is a proper Poincaré section, but it allows the estimation of $\hat{\ell}$.

Because of the hyperchaotic behavior, an implicit technique is used as a reference of comparison to evaluate the synchronization. The correlation between probabilities of recurrence (CPR) [55], an index based on recurrence properties of the system, was chosen and has proven to be effective in assessing phase synchronization in non-phase-coherent dynamics and nonstationary data [55]. Basically, the index is the normalized cross correlation coefficient between the probability of recurrence [Fig. 11(b)] of both systems. When there is phase sync, the amount of recurrence after a τ time lag is approximately the same for both systems and that yields a CPR approximately equal to 1.

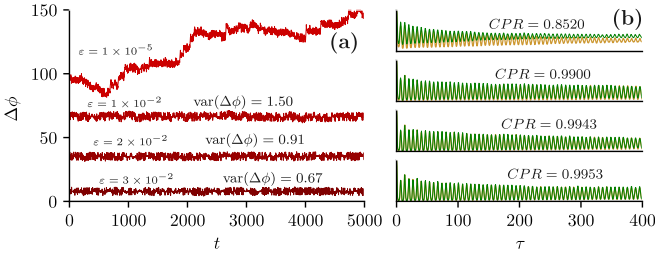

FIG. 11. Two mutually coupled hyperchaotic Rössler oscillators showing the (a) phase difference $\Delta\phi$ and (b) probability of recurrence [55] for four values of coupling strength.

The results in Fig. 11 show that the VFP is in agreement with the CPR index. The stronger the coupling, the greater the CPR index, the smaller the variance of the $\Delta\phi$, and the higher the quality of the synchronized state.

B. Nonlinear oscillators coupled by phase

Here, examples of the VFP-based coupling schemes (Secs. III D and IV) are discussed. Consider the vector fields of two periodic Rössler oscillators

$$\boldsymbol{f}_1 = \begin{bmatrix} -0.8y_1 - z_1 \\ 0.8x_1 + 0.3y_1 \\ 2.0 + z_1(x_1 - 4.0) \end{bmatrix}, \quad \boldsymbol{f}_2 = \begin{bmatrix} -0.9y_2 - z_2 \\ 0.9x_2 + 0.3y_2 \\ 2.0 + z_2(x_2 - 4.0) \end{bmatrix}. \tag{32}$$

In order to phase synchronize both oscillators using the VFP, two configurations of unidirectional coupling ($\beta = 0$) are implemented. The first is given by (11) and considers the full knowledge of the vector field; the second (27) is based on the states of the systems. Theorem 2 is also used for comparison.

Figure 12 shows that (in a steady state) the observed maximum and minimum values of phase difference are very similar for both implementations and remain within the theoretical bounds given by Theorem 2, although these are clearly

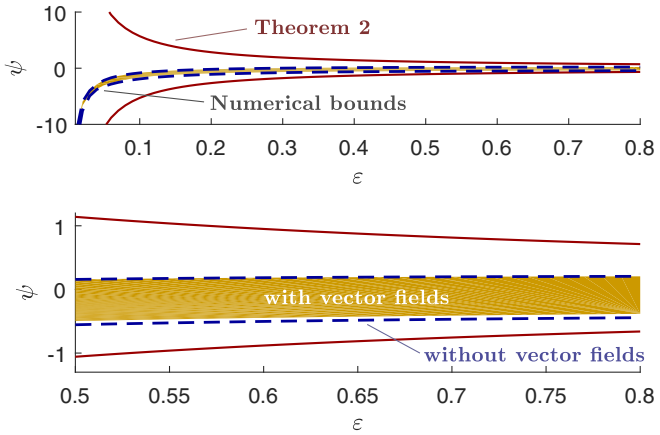

FIG. 12. Bounds of the phase difference ψ for two unidirectionally coupled Rössler oscillators computed by Theorem 2 (red line) and observed numerically, for ten Monte Carlo runs, with (yellow area) and without (blue dashed line) the knowledge of the vector fields, implemented by (11) and (27), respectively. The bottom plot shows a detailed view of the top one.

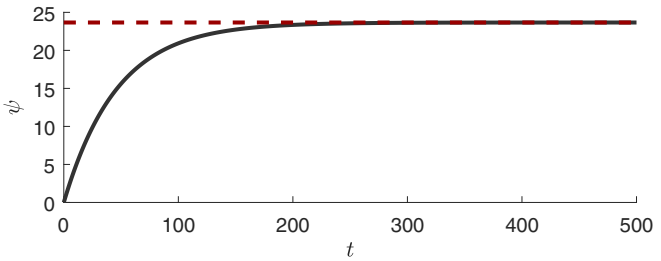

FIG. 13. Time evolution of the phase difference ψ (solid line) and the theoretical strict phase-locking value ψ_{dev} (dashed line), calculated from (20), for mutually coupled cord and van der Pol oscillators as in (11).

conservative for small values of ε. The coupling scheme based on the VFP can also ensure strict phase locking (23) for coupled oscillators with constant norm of the vector fields along the attractor, even for very different oscillators. Consider a van der Pol oscillator (9), with $(\mu,\beta,\omega) = (4,1,1)$, and a periodic cord oscillator (28), with $(a,b,F,G) = (0.258,3.85,8.0,1.0)$, mutually coupled ($\beta = 1$) as in (11). To ensure $\|\boldsymbol{f}_i(\boldsymbol{x}_i)\| = \text{const}\ \forall \boldsymbol{x}_i \in \Gamma_i$, the systems are simulated with $\dot{\boldsymbol{x}} = \alpha_i \boldsymbol{f}_i(\boldsymbol{x}_i)/\|\boldsymbol{f}_i(\boldsymbol{x}_i)\|$, where $\boldsymbol{f}_i(\boldsymbol{x}_i)$ is the original vector field of the systems, $\alpha_1 = 57.369$ (cord), and $\alpha_2 = 2.392$ (van der Pol). Figure 13 shows the time evolution of the phase difference and the computed theoretical strict phase-locking value ψ_{dev}. Clearly, $\psi(t) \to \psi_{\text{dev}}$ as $t \to \infty$.

The results can also be applied to systems with any dimension. Consider, for instance, a van der Pol oscillator ($n = 2$) mutually coupled ($\beta = 1$) with the well-known Hodgkin-Huxley neuronal model ($n = 4$). The van der Pol system is described by (9) with the parameters $(\mu,\beta,\omega) = (3,1,1)$ and the Hodgkin-Huxley model is described in [56], p. 37, with the parameters $(I,C,E_{\text{K}},E_{\text{Na}},E_{\text{L}},\bar{g}_{\text{K}},\bar{g}_{\text{Na}},g_{\text{L}}) = (10,1,-12,120,10.6,36,120,0.3)$. Those are systems with high variance of the vector field norm along the attractor.

Figure 14 shows the results for various coupling strengths. The implementation that uses the knowledge of the vector field (yellow area) remains within the bounds provided in Theorem 1 and the coupling based on the state variables (blue dashed lines) remains close, but not inside the region defined by the theoretical bounds. It was observed (not shown in the figures) that at higher sampling rates the vector field estimates improve and likewise for all subsequent results that depend on such estimation.

VI. CONCLUSION

This work presented a phase definition (VFP) which is clearly related to the zero Lyapunov exponent. The defined phase was proved to be a monotonically increasing function of time (Proposition 1), it is incremented by 2π at every rotating cycle for periodic oscillators (Proposition 3) and it can be applied to a large class of oscillators, of any dimension, because it does not depend on finding a rotation plane or the like.

Illustrative examples have shown that the performance of commonly found phaselike variables (defined by Poincaré

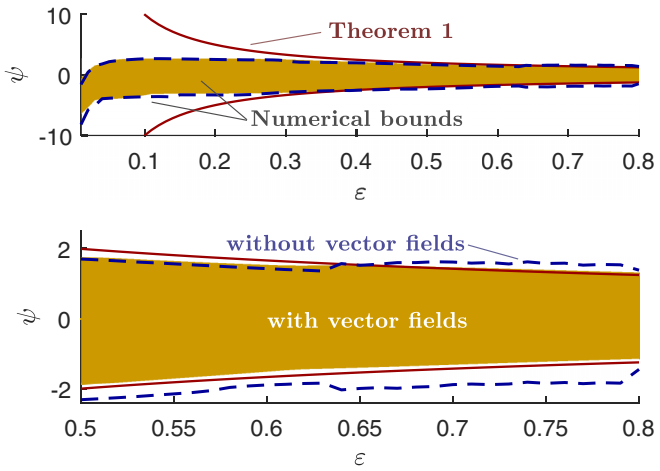

FIG. 14. Bounds of the phase difference ψ for two mutually coupled van der Pol and Hodgkin-Huxley oscillators computed by Theorem 2 (red line) and observed numerically, for ten Monte Carlo runs, with (yellow area) and without (blue dashed line) the knowledge of the vector fields, implemented by (11) and (27), respectively. The bottom plot shows a detailed view of the top one.

sections, angle, and curvature measurements) is equivalent to the proposed definition only for the perfectly circular Poincaré attractor, however they differ considerably for noncircular attractors. One of the benefits of the proposed definition lies in the possibility of describing intracycle phase dynamics with a consistent interpretation related to the zero Lyapunov exponent and at the same time it can be applied to oscillators of any dimension. This allows the comparison of the phase dynamics between very different systems in a meaningful way.

Numerical results with cord and modified Hodgkin-Huxley oscillators showed that the VFP can be used to assess phase synchronization and provide information about the quality of the synchronization, beyond the binary status of yes-no phase sync. Simulations showed that the VFP can be applied when the vector field is unknown and when only one state variable is available. An example with coupled hyperchaotic Rössler oscillators showed that similar results can be obtained for other classes of oscillators.

The proposed VFP also provides insight into the problem of choosing coupling schemes (Secs. III D and IV) to phase synchronize two oscillators and how to effectively maximize the influence on phase dynamics, for a general oscillator. When the equations of the vector fields are known and for a special coupling related to the definition of the VFP, it is possible to ensure strict (20) and (23) and nonstrict (Theorems 1 and 2) phase-locking regimes, with uni- and bidirectional coupling. Although such a special coupling scheme may not be easily implementable in practice, the corresponding synchronization results are taken as confirmations of the consistency of the VFP.

ACKNOWLEDGMENTS

L.F. is grateful to IFMG Campus Betim for an academic leave. L.A.A. and L.A.B.T. gratefully acknowledge financial support from CNPq.

APPENDIX: PROOFS OF PROPOSITIONS AND THEOREMS

Proof of Proposition 1. From (4),

$$\begin{aligned}\phi(t) &= \phi_0 + \int_\gamma c(\boldsymbol{x})\boldsymbol{f}(\boldsymbol{x})d\boldsymbol{x}\\ &= \phi_0 + \int_0^t c(\boldsymbol{x}\circ\tau)\boldsymbol{f}^\top(\boldsymbol{x}\circ\tau).\boldsymbol{f}(\boldsymbol{x}\circ\tau)d\tau\\ &= \phi_0 + \int_0^t c(\boldsymbol{x}\circ\tau)\|\boldsymbol{f}(\boldsymbol{x}\circ\tau)\|^2 d\tau \qquad \text{(A1)}\end{aligned}$$

holds, in which $\|\cdot\|$ denotes the L_2-norm and the trajectory γ was parametrized by τ. Resorting to the second fundamental theorem of calculus, the time derivative of $\phi(t)$ is

$$\frac{d\phi}{dt} = c(\boldsymbol{x})\|\boldsymbol{f}(\boldsymbol{x})\|^2. \qquad \text{(A2)}$$

Since $c(\boldsymbol{x})$ is a positive scalar field for all $\boldsymbol{x} \in X$ (see Definition 1), the time derivative of $\phi(t)$ is always positive and $\phi(t)$ monotonic. ■

Proof of Proposition 3. Assuming $\boldsymbol{x} \in \Gamma_0$, the phase increment during a full period T is

$$\begin{aligned}\phi(T) &= 0 + \int_0^T c(\boldsymbol{x}\circ\tau)\|\boldsymbol{f}(\boldsymbol{x}\circ\tau)\|^2 d\tau\\ &= \int_0^T \frac{2\pi}{\ell\|\boldsymbol{f}(\boldsymbol{x}\circ\tau)\|}\|\boldsymbol{f}(\boldsymbol{x}\circ\tau)\|^2 d\tau\\ &= \frac{2\pi}{\ell}\int_0^T \|\boldsymbol{f}(\boldsymbol{x}\circ\tau)\|d\tau = \frac{2\pi}{\ell}\ell = 2\pi.\end{aligned}$$

■

The following lemma will be useful to prove Theorem 1.

Lemma 1. In the second system in (11), or similarly the first system with $\beta = 1$, for any initial condition $\boldsymbol{x}_{0,2} \in \Gamma_2$ (Assumption 2), the states will remain on the attractor $\boldsymbol{x}_2(t;\boldsymbol{x}_{0,2}) \in \Gamma_2$ for all $t > 0$.

Proof. The attractor Γ_2 can be understood as an $\boldsymbol{f}_2$-invariant manifold, since the unperturbed motion ($\varepsilon = 0$) yields $\boldsymbol{x}_2(t;\boldsymbol{x}_{0,2}) \in \Gamma_2\ \forall t > 0$ (Assumption 1). For a given initial condition $\boldsymbol{x}_{0,2} \in \Gamma_2$ of the perturbed motion ($\varepsilon \neq 0$), the trajectory will remain on the attractor Γ_2 if it is also $\hat{\boldsymbol{f}}_2$ invariant, where $\hat{\boldsymbol{f}}_2 := \boldsymbol{f}_2(\boldsymbol{x}_2) + \varepsilon\boldsymbol{f}_2(\boldsymbol{x}_2)\psi$. It can be done by verifying if the Lie bracket between both vector fields, perturbed and unperturbed, vanishes:

$$\begin{aligned}[\boldsymbol{f}_2,\hat{\boldsymbol{f}}_2] &= \frac{d^\top\hat{\boldsymbol{f}}_2}{d\boldsymbol{x}_2}\boldsymbol{f}_2 - \frac{d^\top\boldsymbol{f}_2}{d\boldsymbol{x}_2}\hat{\boldsymbol{f}}_2,\\ &= \frac{d^\top[\boldsymbol{f}_2+\varepsilon\boldsymbol{f}_2\psi]}{d\boldsymbol{x}_2}\boldsymbol{f}_2 - \frac{d^\top\boldsymbol{f}_2}{d\boldsymbol{x}_2}[\boldsymbol{f}_2+\varepsilon\boldsymbol{f}_2\psi],\\ &= \frac{d^\top\boldsymbol{f}_2}{d\boldsymbol{x}_2}\boldsymbol{f}_2 + \varepsilon\psi\frac{d^\top\boldsymbol{f}_2}{d\boldsymbol{x}_2}\boldsymbol{f}_2\\ &\quad - \frac{d^\top\boldsymbol{f}_2}{d\boldsymbol{x}_2}\boldsymbol{f}_2 - \varepsilon\psi\frac{d^\top\boldsymbol{f}_2}{d\boldsymbol{x}_2}\boldsymbol{f}_2,\\ &= \varepsilon\psi\left[\frac{d^\top\boldsymbol{f}_2}{d\boldsymbol{x}_2}\boldsymbol{f}_2 - \frac{d^\top\boldsymbol{f}_2}{d\boldsymbol{x}_2}\boldsymbol{f}_2\right] = 0, \qquad \text{(A3)}\end{aligned}$$

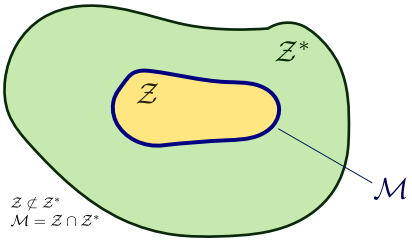

FIG. 15. Representation of the sets $\mathcal{M}$, $\mathcal{Z}$, and $\mathcal{Z}^*$.

where explicit dependences of $\boldsymbol{x}_2$ were omitted. Then the manifold Γ_2 is involutive (since it is integrable) and invariant under the proposed perturbation, which means that the perturbed motion will remain on the attractor Γ_2 for all $t > 0$. ■

Proof of Theorem 1. For the sake of clarity, some explicit dependences of $\boldsymbol{x}_1$ and $\boldsymbol{x}_2$ will be suppressed. First, without loss of generality, let us consider the translated system with $\bar{\psi} := \psi - \psi_{\min}$, with $\psi_{\min}$ a constant value given by (18), where the new complete state vector is $\bar{\boldsymbol{x}} := [\boldsymbol{x}_1^\top, \boldsymbol{x}_2^\top, \bar{\psi}]^\top$. Concerning the mutually coupled ($\beta = 1$) case given by (11), one can take the positive semidefinite V function $V(\bar{\boldsymbol{x}}) = (1/2)(\bar{\psi})^2$, where its time derivative is given by

$$\dot{V} = \left[\frac{2\pi}{\ell_1}\|\boldsymbol{f}_1\||1-\varepsilon\psi| - \frac{2\pi}{\ell_2}\|\boldsymbol{f}_2\||1+\varepsilon\psi|\right]\bar{\psi}. \quad \text{(A4)}$$

By analyzing the signal of $\dot{V}$ in (A4), it will be convenient to define the following sets:

$$\mathcal{Z} = \left\{\bar{\boldsymbol{x}} \in \mathbb{R}^{n_1+n_2+1} : 0 \leqslant \bar{\psi} \leqslant \frac{1}{\varepsilon}\left(\frac{\ell_2\|\boldsymbol{f}_1\| - \ell_1\|\boldsymbol{f}_2\|}{\ell_2\|\boldsymbol{f}_1\| + \ell_1\|\boldsymbol{f}_2\|}\right) - \psi_{\min}, \boldsymbol{x}_1 \in \Gamma_1, \boldsymbol{x}_2 \in \Gamma_2\right\} \quad \text{(A5)}$$

and

$$\mathcal{Z}^* = \left\{\bar{\boldsymbol{x}} \in \mathbb{R}^{n_1+n_2+1} : -\frac{1}{\varepsilon} - \psi_{\min} \leqslant \bar{\psi} \leqslant 0 \text{ or } \frac{1}{\varepsilon}\left(\frac{\ell_2\|\boldsymbol{f}_1\| - \ell_1\|\boldsymbol{f}_2\|}{\ell_2\|\boldsymbol{f}_1\| + \ell_1\|\boldsymbol{f}_2\|}\right) - \psi_{\min} \leqslant \bar{\psi} \leqslant \frac{1}{\varepsilon} - \psi_{\min}, \boldsymbol{x}_1 \in \Gamma_1, \boldsymbol{x}_2 \in \Gamma_2\right\}. \quad \text{(A6)}$$

Note that there exists a nonempty intersection of $\mathcal{Z}$ and $\mathcal{Z}^*$,

$$\mathcal{M} = \left\{\bar{\boldsymbol{x}} \in \mathbb{R}^{n_1+n_2+1} : \bar{\psi} = 0 \text{ or } \bar{\psi} = \frac{1}{\varepsilon}\left(\frac{\ell_2\|\boldsymbol{f}_1\| - \ell_1\|\boldsymbol{f}_2\|}{\ell_2\|\boldsymbol{f}_1\| + \ell_1\|\boldsymbol{f}_2\|}\right) - \psi_{\min}, \boldsymbol{x}_1 \in \Gamma_1, \boldsymbol{x}_2 \in \Gamma_2\right\}, \quad \text{(A7)}$$

where $\mathcal{M} \equiv \mathcal{Z} \cap \mathcal{Z}^*$ ($\not\equiv \emptyset$) and $\mathcal{M} \not\equiv \mathcal{Z}^*$ ($\mathcal{Z}^* \setminus \mathcal{M} \not\equiv \emptyset$), as represented in Fig. 15. Because of (12), it is also possible to say that $\mathcal{M} \not\equiv \mathcal{Z}$ ($\mathcal{Z} \setminus \mathcal{M} \not\equiv \emptyset$).

By analyzing (A4), the conditions (see [50], p. 29, as well as [57]) (i) $V(\boldsymbol{x}) \geqslant a(\|\bar{\psi}\|)$, e.g., $a(\|\bar{\psi}\|) := \frac{1}{2}\|\bar{\psi}\|$; (ii) $\dot{V}(\boldsymbol{x}) = 0$ ($\boldsymbol{x} \in \mathcal{M}$) and $\dot{V}(\boldsymbol{x}) < 0$ ($\boldsymbol{x} \notin \mathcal{M}$); and (iii) $\mathcal{M}$ contains no entire semitrajectories for $t \in [0,\infty)$ hold for all $\bar{\boldsymbol{x}} \in \mathcal{Z}^*$. These condition were stated by Risito [57] as sufficient conditions for partial stability ($\bar{\psi}$ stability), where $\text{dist}(\bar{\boldsymbol{x}},\mathcal{M}) \to 0$ as $t \to \infty$. So, in light of Definitions 3 and 4, the set $\mathcal{Z}$ can be called invariant and attractive, because it is surrounded by an attractive set $\mathcal{Z}^*$.

Because of Lemma 1 and Assumption 2, $\boldsymbol{x}_1 \in \Gamma_1$ and $\boldsymbol{x}_2 \in \Gamma_2$ will hold for all $t \geqslant 0$. Because of Assumption 3, the initial phase difference can be $\psi_0 \in (-1/\varepsilon, 1/\varepsilon) \Rightarrow \psi_0 \in \mathcal{Z} \cup \mathcal{Z}^*$, i.e., already inside the attractive set or its basin of attraction.

The bounds given in (18) and (19) clearly take the worst cases (upper and lower bounds) of $\bar{\psi}$ when $\boldsymbol{x} \in \mathcal{Z}$ [see Eq. (12)]. Because the set $\mathcal{Z}$ is invariant and its neighborhood complies with the $\bar{\psi}$-stability condition, the nonstrict phase locking $\psi_{\min} \leqslant \psi \leqslant \psi_{\max}\ \forall t \geqslant t_0$ will hold for some $t_0 < \infty$. This completes the proof. ■

The result (20) can be demonstrated as follows. In the special case where the norm of the vector fields is constant, i.e., $\|\boldsymbol{f}_i(\boldsymbol{x}_i)\| = v_i\ \forall \boldsymbol{x}_i \in \Gamma_i$ for $i \in \{1,2\}$, and concerning the bidirectionally coupled case ($\beta = 1$), part of (11) can be simplified as

$$\dot{\psi} = \frac{2\pi}{\ell_1}v_1|1-\psi| - \frac{2\pi}{\ell_2}v_2|1+\psi|, \quad \text{(A8)}$$

which allows the evaluation of the stability of ψ independent of the state variables $\boldsymbol{x}_1$ and $\boldsymbol{x}_2$. By evaluating (A8), there are two fixed points

$$\dot{\psi}_1^* = \frac{1}{\varepsilon}\left(\frac{\ell_2 v_1 - \ell_1 v_2}{\ell_2 v_1 + \ell_1 v_2}\right), \quad \text{(A9)}$$

$$\dot{\psi}_2^* = \frac{1}{\varepsilon}\left(\frac{\ell_2 v_1 + \ell_1 v_2}{\ell_2 v_1 - \ell_1 v_2}\right), \quad \text{(A10)}$$

where (A9) is stable and (A10) is unstable. Because of Assumption 3, the initial phase difference is inside the basin of attraction of the stable fixed point, leading to an asymptotic convergence to (20) as $t \to \infty$.

The unidirectionally coupled case follows the same reasoning that has been shown so far. Therefore, the following proofs will refer to the ones presented above.

Proof of Theorem 2. Concerning the unidirectionally coupled ($\beta = 0$) case (11) and following the procedure in the proof of Theorem 1, it is possible to define a similar V function $V(\bar{\boldsymbol{x}}) = (1/2)(\bar{\psi})^2$, where $\bar{\psi} := \psi - \psi_{\min}$, but with $\psi_{\min}$ given by (21). The time derivative of V is

$$\dot{V} = \left[\frac{2\pi}{\ell_1}\|\boldsymbol{f}_1\| - \frac{2\pi}{\ell_2}\|\boldsymbol{f}_2\||1+\varepsilon\psi|\right]\bar{\psi}. \quad \text{(A11)}$$

By analyzing the signal of $\dot{V}$ in (A11), the sets $\mathcal{Z}$, $\mathcal{Z}^*$, and $\mathcal{M}$ can be defined respectively as

$$\mathcal{Z} = \left\{\bar{\boldsymbol{x}} \in \mathbb{R}^{n_1+n_2+1} : 0 \leqslant \bar{\psi} \leqslant \frac{1}{\varepsilon}\left(\frac{\ell_2\|\boldsymbol{f}_1\|}{\ell_1\|\boldsymbol{f}_2\|} - 1\right) - \psi_{\min}, \boldsymbol{x}_1 \in \Gamma_1, \boldsymbol{x}_2 \in \Gamma_2\right\}, \quad \text{(A12)}$$

$$\mathcal{Z}^* = \Big\{\bar{\boldsymbol{x}} \in \mathbb{R}^{n_1+n_2+1} : -\frac{1}{\varepsilon} - \psi_{\min} \leqslant \bar{\psi} \leqslant 0 \text{ or } \frac{1}{\varepsilon}\left(\frac{\ell_2\|\boldsymbol{f}_1\|}{\ell_1\|\boldsymbol{f}_2\|} - 1\right) - \psi_{\min} \leqslant \bar{\psi} < \infty, \boldsymbol{x}_1 \in \Gamma_1, \boldsymbol{x}_2 \in \Gamma_2\Big\}, \tag{A13}$$

$$\mathcal{M} = \Big\{\bar{\boldsymbol{x}} \in \mathbb{R}^{n_1+n_2+1} : \bar{\psi} = 0 \text{ or } \bar{\psi} = \frac{1}{\varepsilon}\left(\frac{\ell_2\|\boldsymbol{f}_1\|}{\ell_1\|\boldsymbol{f}_2\|} - 1\right) - \psi_{\min}, \boldsymbol{x}_1 \in \Gamma_1, \boldsymbol{x}_2 \in \Gamma_2\Big\}. \tag{A14}$$

Using these sets and replacing Assumption 3 by Assumption 4, it is possible to make the same reasoning stated in the proof of Theorem 1 and conclude that the bounds given in (21) and (22) take the wort cases (upper and lower bounds), where the nonstrict phase-locking condition (14) holds for some finite time.

This completes the proof. ■

The result (23) can be demonstrated as follows. In the special case where the norm of the vector fields are constant, i.e., $\|\boldsymbol{f}_i(\boldsymbol{x}_i)\| = v_i \; \forall \boldsymbol{x}_i \in \Gamma_i$ for $i \in \{1,2\}$, and concerning the unidirectionally coupled case ($\beta = 0$), Eq. (11) becomes

$$\dot{\psi} = \frac{2\pi}{\ell_1}v_1 - \frac{2\pi}{\ell_2}v_2|1+\psi|, \tag{A15}$$

which allows the evaluation of the stability of ψ independent of the state variables $\boldsymbol{x}_1$ and $\boldsymbol{x}_2$. By evaluating (A8), there are two fixed points

$$\dot{\psi}_1^* = \frac{1}{\varepsilon}\left(\frac{\ell_2 v_1}{\ell_1 v_2} - 1\right), \tag{A16}$$

$$\dot{\psi}_2^* = -\frac{1}{\varepsilon}\left(\frac{\ell_2 v_1}{\ell_1 v_2} + 1\right), \tag{A17}$$

where (A16) is stable and (A17) is unstable. The main difference here from the bidirectional case is that the unstable fixed point $\dot{\psi}_2^*$ (A17) is always negative, which allows any positive initial condition $\psi_0 > 0$ to converge to $\dot{\psi}_1^*$ as $t \to \infty$. The same is true for any initial condition stated by Assumption 4, which ensures the asymptotic convergence to (23).

[1] H. Nakao, Contemp. Phys. **57**, 188 (2016).
[2] A. T. Winfree, J. Theor. Biol. **16**, 15 (1967).
[3] Y. Kuramoto, *Chemical Oscillations, Waves, and Turbulence* (Springer, New York, 1984).
[4] S. H. Strogatz, Nature (London) **410**, 268 (2001).
[5] H. Fujisaka and T. Yamada, Prog. Theor. Phys. **69**, 32 (1983).
[6] L. M. Pecora and T. L. Carroll, Phys. Rev. Lett. **64**, 821 (1990).
[7] S. Boccaletti, J. Kurths, G. Osipov, D. Valladares, and C. Zhou, Phys. Rep. **366**, 1 (2002).
[8] A. S. Pikovsky, M. G. Rosenblum, G. V. Osipov, and J. Kurths, Physica D **104**, 219 (1997).
[9] G. V. Osipov, B. Hu, C. Zhou, M. V. Ivanchenko, and J. Kurths, Phys. Rev. Lett. **91**, 024101 (2003).
[10] M. G. Rosenblum, A. S. Pikovsky, J. Kurths, C. Schafer, and P. A. Tass, Handb. Biol. Phys. **4**, 279 (2003).
[11] T. Pereira, M. S. Baptista, and J. Kurths, Phys. Rev. E **75**, 026216 (2007).
[12] R. Follmann, E. E. N. Macau, and E. Rosa, Phys. Lett. A **373**, 2146 (2009).
[13] M. Bonnin, F. Corinto, and M. Gilli, Int. J. Bifurcat. Chaos Appl. Sci. Eng. **20**, 645 (2010).
[14] J. T. C. Schwabedal and A. S. Pikovsky, Eur. Phys. J.: Spec. Top. **187**, 63 (2010).
[15] J. T. C. Schwabedal, A. S. Pikovsky, B. Kralemann, and M. G. Rosenblum, Phys. Rev. E **85**, 026216 (2012).
[16] Y. Zou, R. V. Donner, and J. Kurths, Chaos **22**, 013115 (2012).
[17] R. Follmann, E. Rosa, E. E. N. Macau, and J. R. C. Piqueira, Int. J. Bifurcation Chaos **23**, 1350179 (2013).
[18] P. T. Clemson and A. Stefanovska, Phys. Rep. **542**, 297 (2014).
[19] A. S. Pikovsky, M. Zaks, M. G. Rosenblum, G. Osipov, and J. Kurths, Chaos **7**, 680 (1997).
[20] B. Blasius and L. Stone, Int. J. Bifurcation Chaos **10**, 2361 (2000).
[21] V. Anishchenko, V. Astakhov, A. Neiman, T. Vadivasova, and L. Schimansky-Geier, *Nonlinear Dynamics of Chaotic and Stochastic Systems: Tutorial and Modern Developments*, Springer Series in Synergetics (Springer-Verlag, Berlin Heidelberg, New York, 2007).
[22] Y. F. Suprunenko, P. T. Clemson, and A. Stefanovska, Phys. Rev. E **89**, 012922 (2014).
[23] A. E. Hramov, A. A. Koronovskii, M. K. Kurovskaya, and O. I. Moskalenko, Chaos Soliton. Fract. **78**, 118 (2015).
[24] B. Kralemann, L. Cimponeriu, M. G. Rosenblum, A. S. Pikovsky, and R. Mrowka, Phys. Rev. E **77**, 066205 (2008).
[25] H. Haken, Phys. Lett. **94**, 71 (1983).
[26] T. Yalçinkaya and Y.-C. Lai, Phys. Rev. Lett. **79**, 3885 (1997).
[27] E. F. Stone, Phys. Lett. A **163**, 367 (1992).
[28] A. Pikovsky, M. Rosenblum, and J. Kurths, Int. J. Bifurcation Chaos **10**, 2291 (2000).
[29] J. Y. Chen, K. W. Wong, and J. W. Shuai, Phys. Lett. A **285**, 312 (2001).
[30] A. S. Pikovsky, M. G. Rosenblum, and J. Kurths, *Synchronization: A Universal Concept in Nonlinear Sciences* (Cambridge University Press, Cambridge, 2003).
[31] L. A. Aguirre and C. Letellier, Phys. Rev. E **83**, 066209 (2011).
[32] D. Li, Phys. Lett. A **372**, 387 (2008).
[33] J. Kurths, M. C. Romano, M. Thiel, G. V. Osipov, M. V. Ivanchenko, I. Z. Kiss, and J. L. Hudson, Nonlinear Dyn. **44**, 135 (2006).
[34] M. G. Rosenblum, A. S. Pikovsky, and J. Kurths, Phys. Rev. Lett. **76**, 1804 (1996).
[35] M. Le Van Quyen, J. Foucher, J. Lachaux, E. Rodriguez, A. Lutz, J. Martinerie, and F. J. Varela, J. Neurosci. Methods **111**, 83 (2001).
[36] A. E. Hramov and A. A. Koronovskii, Physica D **206**, 252 (2005).
[37] M. T. Ferreira, C. B. Nóbrega Freitas, M. O. Domingues, and E. E. N. Macau, Chaos **25**, 013117 (2015).
[38] M. S. Baptista, T. Pereira, and J. Kurths, Physica D **216**, 260 (2006).

[39] K. Josić and D. J. Mar, Phys. Rev. E **64**, 056234 (2001).
[40] M. Beck and K. Josić, Chaos **13**, 247 (2003).
[41] S. Strogatz, *Nonlinear Dynamics And Chaos* (Sarat Book House, Delhi, 2007).
[42] L. Glass and M. Mackey, *From Clocks to Chaos: The Rhythms of Life* (Princeton University Press, Princeton, 1988).
[43] B. van der Pol, Philos. Mag. **3**, 65 (1927).
[44] L. A. Aguirre and L. Freitas, Nonlinear Dyn. **91**, 2203 (2018).
[45] J. R. C. Piqueira, Commun. Nonlinear Sci. Numer. Simul. **16**, 3844 (2011).
[46] X. Zhang, X. Hu, J. Kurths, and Z. Liu, Phys. Rev. E **88**, 010802 (2013).
[47] C. Xu, Y. Sun, J. Gao, T. Qiu, Z. Zheng, and S. Guan, Sci. Rep. **6**, 21926 (2016).
[48] C. Chicone, *Ordinary Differential Equations with Applications* (Springer, New York, 2006).
[49] G. V. Osipov, J. Kurths, and C. Zhou, *Synchronization in Oscillatory Networks*, Springer Series in Synergetics (Springer, Berlin, 2007).
[50] V. Vorotnikov, *Partial Stability and Control*, 1st ed. (Birkhäuser, Boston, 1997).
[51] I. V. Miroshnik, Automatica **40**, 473 (2004).
[52] F. Takens, in *Dynamical Systems and Turbulence, Warwick, 1980*, edited by D. Rand and L.-S. Young (Springer, Berlin, 1981), pp. 366–381.
[53] H. A. Braun, M. T. Huber, M. Dewald, K. Schäfer, and K. Voigt, Int. J. Bifurcat. Chaos **08**, 881 (1998).
[54] U. Feudel, A. Neiman, X. Pei, W. Wojtenek, H. Braun, M. Huber, and F. Moss, Chaos **10**, 231 (2000).
[55] M. C. Romano, M. Thiel, J. Kurths, I. Z. Kiss, and J. L. Hudson, Europhys. Lett. **71**, 466 (2005).
[56] E. M. Izhikevich, *Dynamical Systems in Neuroscience: The Geometry of Excitability and Bursting* (MIT Press, Cambridge, 2007).
[57] C. Risito, Ann. Mat. Pura Appl. Ser. 4 **84**, 279 (1970).